NASA/TM—2013-216586

Characterization and Comparison of Vibration Transfer Paths in a Helicopter Gearbox and a Fixture Mounted Gearbox

Anwarul Islam
Youngstown State University, Youngstown, Ohio

Paula Dempsey
Glenn Research Center, Cleveland, Ohio

Jason Feldman and Chris Larsen
Etegent Technologies, Ltd., Cincinnati, Ohio

September 2013

NASA STI Program . . . in Profile

Since its founding, NASA has been dedicated to the advancement of aeronautics and space science. The NASA Scientific and Technical Information (STI) program plays a key part in helping NASA maintain this important role.

The NASA STI Program operates under the auspices of the Agency Chief Information Officer. It collects, organizes, provides for archiving, and disseminates NASA's STI. The NASA STI program provides access to the NASA Aeronautics and Space Database and its public interface, the NASA Technical Reports Server, thus providing one of the largest collections of aeronautical and space science STI in the world. Results are published in both non-NASA channels and by NASA in the NASA STI Report Series, which includes the following report types:

- TECHNICAL PUBLICATION. Reports of completed research or a major significant phase of research that present the results of NASA programs and include extensive data or theoretical analysis. Includes compilations of significant scientific and technical data and information deemed to be of continuing reference value. NASA counterpart of peer-reviewed formal professional papers but has less stringent limitations on manuscript length and extent of graphic presentations.

- TECHNICAL MEMORANDUM. Scientific and technical findings that are preliminary or of specialized interest, e.g., quick release reports, working papers, and bibliographies that contain minimal annotation. Does not contain extensive analysis.

- CONTRACTOR REPORT. Scientific and technical findings by NASA-sponsored contractors and grantees.

- CONFERENCE PUBLICATION. Collected papers from scientific and technical conferences, symposia, seminars, or other meetings sponsored or cosponsored by NASA.

- SPECIAL PUBLICATION. Scientific, technical, or historical information from NASA programs, projects, and missions, often concerned with subjects having substantial public interest.

- TECHNICAL TRANSLATION. English-language translations of foreign scientific and technical material pertinent to NASA's mission.

Specialized services also include creating custom thesauri, building customized databases, organizing and publishing research results.

For more information about the NASA STI program, see the following:

- Access the NASA STI program home page at *http://www.sti.nasa.gov*

- E-mail your question to *help@sti.nasa.gov*

- Fax your question to the NASA STI Information Desk at 443–757–5803

- Phone the NASA STI Information Desk at 443–757–5802

- Write to:
  STI Information Desk
  NASA Center for AeroSpace Information
  7115 Standard Drive
  Hanover, MD 21076–1320

NASA/TM—2013-216586

Characterization and Comparison of Vibration Transfer Paths in a Helicopter Gearbox and a Fixture Mounted Gearbox

Anwarul Islam
Youngstown State University, Youngstown, Ohio

Paula Dempsey
Glenn Research Center, Cleveland, Ohio

Jason Feldman and Chris Larsen
Etegent Technologies, Ltd., Cincinnati, Ohio

National Aeronautics and
Space Administration

Glenn Research Center
Cleveland, Ohio 44135

September 2013

Acknowledgments

The authors would like to express their sincere gratitude to the U.S. Army Aviation Engineering Directorate and NASA Glenn Research Center for supporting data collection on the AH-64 helicopter and on the nose gearbox fixture, respectively.

This work was sponsored by the Fundamental Aeronautics Program at the NASA Glenn Research Center.

Level of Review: This material has been technically reviewed by technical management.

Available from

NASA Center for Aerospace Information
7115 Standard Drive
Hanover, MD 21076–1320

National Technical Information Service
5301 Shawnee Road
Alexandria, VA 22312

Available electronically at http://www.sti.nasa.gov

Characterization and Comparison of Vibration Transfer Paths in a Helicopter Gearbox and a Fixture Mounted Gearbox

Anwarul Islam
Youngstown State University
Youngstown, Ohio 44555

Paula Dempsey
National Aeronautics and Space Administration
Glenn Research Center
Cleveland, Ohio 44135

Jason Feldman and Chris Larsen
Etegent Technologies, Ltd.
Cincinnati, Ohio 45212

Abstract

Health monitoring of rotorcraft components, currently being performed by Health and Usage Monitoring Systems through analyses of vibration signatures of dynamic mechanical components, is very important for their safe and economic operation. HUMS analyze vibration signatures associated with faults and quantify them as condition indicators to predict component behavior. Vibration transfer paths are characterized by frequency response functions derived from the input/output relationship between applied force and dynamic response through a structure as a function of frequency. With an objective to investigate the differences in transfer paths, transfer path measurements were recorded under similar conditions in the left and right nose gearboxes of an AH-64 helicopter and in an isolated left nose gearbox in a test fixture at NASA Glenn Research Center. The test fixture enabled the application of measured torques—common during an actual operation. An impact hammer as well as commercial and lab piezo shakers, were used in conjunction with two types of commercially available accelerometers to collect the vibration response under various test conditions. The frequency response functions measured under comparable conditions of both systems were found to be consistent. Measurements made on the fixture indicated certain real-world installation and maintenance issues, such as sensor alignments, accelerometer locations and installation torques, had minimal effect. However, gear vibration transfer path dynamics appeared to be somewhat dependent on the presence of oil, and the transfer path dynamics were notably different if the force input was on the internal ring gear rather than on the external gearbox case.

Introduction

The integrity of the helicopter transmission system is critical to helicopter safety because helicopters depend on the powertrain for propulsion, lift and maneuvering (Ref. 1). A study of 1,168 helicopter accidents from 1990 to 1996 found that accidents due to various system and structural failures were second in importance only to failures due to human causes (Ref. 2). In 1999, 28 out of 192 turbine powered helicopter accidents in the world were directly caused by mechanical failures in the drive train of the propulsion system (Ref. 3). In order to reduce the occurrence of such accidents, the study in Reference 2 recommended the design of Health and Usage Monitoring System (HUMS) capable of predicting impending equipment failure for on-condition maintenance, and more advanced systems capable of warning pilots of imminent equipment failure.

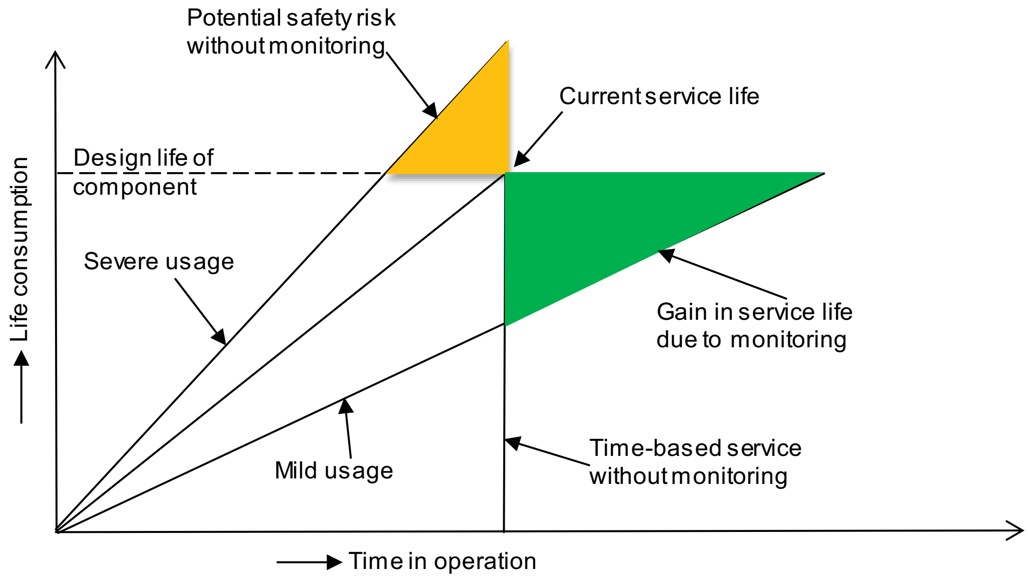

Figure 1.—Economic and safety benefits of health monitoring systems (Ref. 4).

Figure 1 shows the potential safety and economic benefit of diagnostic and prognostic maintenance of critical components in a mechanical system (Ref. 4). If the damage and wear due to usage is more severe than what is expected from the predicted service life of a component, health and usage monitoring would provide a safety benefit. Conversely, the service life could be extended if actual usage is less severe than predicted.

HUMS use algorithms referred to as condition indicators (CIs), which are generated from fault patterns produced in vibration signatures when damaged components interact with their environment. Understanding structural differences between systems may provide insight into the difference in performance of diagnostic tools between such systems.

Damage progression tests of spiral bevel gears, that consist of a ring gear and pinion set, are being performed in the Spiral Bevel Gear Fatigue test rig at the at NASA Glenn Research Center (GRC). The objective of these tests, as outlined in Reference 5, are to determine if ‘seeded or accelerated fault’ tests, in which a component is tested with a known fault, can be used as evidence that a HUMS condition indicator will reliably detect tooth damage when installed on a helicopter. For this approach, existing in-service HUMS flight data from helicopter nose gearbox (NGB) spiral bevel gears will be compared to test rig spiral bevel gear failure progression data. The field data analysis of spiral bevel gears condition indicators determined the CIs that performed the best in the field. The information learned from this analysis, documented in References 6 and 7, was fed into development of the spiral bevel gear rig tests. Performing these tests will also be used to identify the limitations of seeded fault data sets for demonstrating helicopter CI performance.

In addition to performing dynamic tests of the gears with varying levels of damage to the gear teeth, measurements will be made to characterize differences in the structural dynamics between the helicopter and test rig systems. Although the transfer path can change under dynamic conditions due to load and speed, the static structure can also filter the response between the vibration source and the accelerometer on the housing. Understanding how the response of the gear set, at gear mesh due to damage, travels through the structure may answer some questions as to why diagnostic tools perform differently on different systems.

Figure 2.—Three spiral bevel geared systems

The approach used to assess the usefulness of vibration transfer paths in assessing CI performance was to take measurements on three spiral bevel geared systems for comparison. These three systems were the helicopter NGB, a NGB removed from a helicopter and installed in a static fixture, and the spiral bevel gear fatigue rig as shown in Figure 2. This comparison requires taking measurements on the helicopter or fixture that can be compared to future measurements on the test rig. The helicopter nose gearbox transfer path measurements were taken for selecting enveloping/demodulation frequency bands for bearing monitoring (Ref. 8). Since the purpose of measurements made for this analysis was to determine if transfer path measurements under static gear conditions could provide insight into gear CI performance, additional measurements were required (Ref. 9). Limited accessibility to the gear mesh within the NGB installed on the helicopter made it impossible to simulate an impact of the gear teeth at the source. That is, the ideal force input location for this measurement would be directly between meshing gear teeth, but this is not physically possible. However, external measurements made on the helicopter could be repeated on the fixture to verify both had similar response, then additional measurements could be made on the fixture under conditions that could be later compared to the test rig.

The objectives of this research were to compare frequency response functions for a nose gearbox installed on an AH-64 helicopter to those of a left NGB installed in a fixture at GRC for testing and research. The NGB test fixture enabled the application of measured torques—common during an actual operation and the simulation of other environmental conditions experienced in the field that could not be made on the helicopter. Measurements were taken under varying operational conditions and compared on the NGB fixture. This approach first required the comparison of external measurements made on the helicopter to external measurements made on the fixture under the same conditions. Next, measurements taken with the fixture NGB under load and other varying operational conditions were compared. Third, measurements were taken and compared while impacting the gear set near mesh to simulate gear meshing dynamics.

Test Procedure

Modal analysis is generally done to identify the resonance frequencies or natural frequencies of a structure. It is typically performed by exciting a structure with a known force and measuring the vibration response, such as acceleration, at various locations on the structure. Frequency response functions (FRF) are used to analyze structural dynamics under static conditions and to estimate modal parameters for analysis of mechanical systems. An FRF is measured response normalized by measured input. Presence of damage in a dynamic mechanical system is usually reflected in its dynamic vibration signatures. The effect the static structure has on the response can be further analyzed using FRFs. Therefore, vibration transfer path (VTP) characteristics in a NGB might be useful in determining the difference in structural dynamics between the Spiral Bevel Gear Test Rig and a helicopter. In this research, vibration response of left and right NGBs in an AH-64 helicopter and the left NGB in the test fixture at GRC were collected under similar boundary conditions to determine the characteristics of their vibration transfer paths using

FRFs. The similarity between the FRFs of the NGBs in the helicopter and the test fixture were quantified using Kolmogorov-Smirnov tests. Vibration transfer path measurements were recorded on the left and right NGBs of an AH-64 helicopter during the week of April 11 through April 15, 2011, at Fort Campbell, Kentucky (Ref. 8). These measurements were made from 0 to 50 kHz. Since the reaction-mass shaker only provides good excitation from about 3 kHz and up, impact testing was done to measure the low frequency response. These measurements were put together to produce a complete FRF from 0 to 50 kHz; stitching the FRFs together provides a further check that measurements from two different input sources agree. There were six excitation locations in both the left and right NGBs, as shown in Figure 3. These locations were kept as identical as possible in the right NGBs in the helicopter and the left NGB in the test fixture.

Vibration transfer path measurements were also recorded on an isolated left NGB at GRC test facility from April 18 to 20, 2012. The transfer paths were recorded from 0 to 50 kHz. Locations of accelerometers were kept the same on the lab fixture as they were on the helicopter. For comparison, it was important to use the same equipment and locations that were used during the helicopter data collections. Although the measurements in the field were taken with no load on the gear set, the test fixture enabled the application of torque to the input side of the NGB comparable to the torques applied by their engine (Ref. 10).

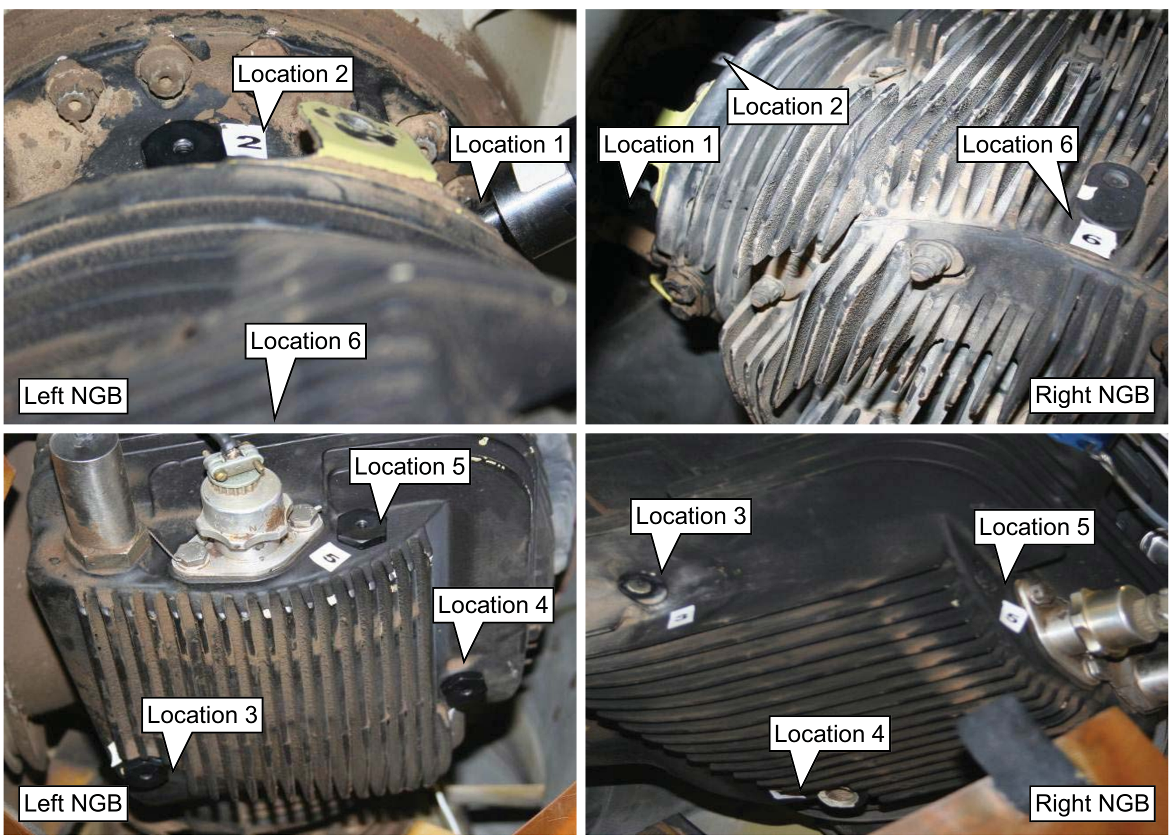

Figure 3.—Shaker locations 1 through 6 on left and right NGBs in AH-64 helicopter.

The basic component of these tests was a 60-sec data set recorded with two shakers one at a time stepping from 0 to 50 kHz in a 5 sec chirp. In this way, each FRF was computed by averaging 12 sweeps. Table I shows the types of shaker and accelerometer, shaker locations and load on gearboxes for each test. However, Test 4 was discarded because the shaker did not function properly. The Commercial Shaker is a piezoelectric actuator and the Lab Piezo Shaker is a custom shaker made from two miniature multilayer Piezo stack actuators and a similarly sized tungsten cube (for reaction mass), which can be seen along with the PCB (Ref. 11) Hammer in Figure 4. While the Commercial Shaker was mounted on the outside of the gearbox, the Lab Piezo Shaker was attached to the ring gear of the NGB close to the gear mesh, since the Commercial Shaker would not fit inside the closed gearbox. For low frequency measurements, a general purpose impact hammer was used since the shakers do not generate much energy below 5 kHz. The left NGB at GRC was also subjected to various ranges of loads, as shown in Table II, to determine if load causes any difference in VTP. Pictures of shaker locations, ring gear, left NGB fixture and the torque application are shown in Figure 5.

TABLE I.—DESCRIPTIONS OF TESTS WITH SHAKER AND ACCELEROMETER TYPES

Test	Shaker type	Accelerometer type	Shaker location	Loads on gearbox/comments
Test 1	Commercial	Dytran	Location 1	Gearbox under range of loads
Test 2	Hammer	Dytran	Location 1	Low frequency component of Test 1
Test 3	Commercial	Dytran	All locations	Gearbox at 4 percent load
Test 4	Lab	Dytran	Ring gear	Shaker faulty, test not used
Test 5[a]	Lab	Dytran	Ring gear	Range of loads, HUMS acc. clocked
Test 6	Lab	PCB HF	Ring gear	Gearbox with oil under range of loads
Test 7	Commercial and Lab	PCB HF	Ring gear	Two additional acc. on ring gear
Test 8	Lab	Dytran	Ring gear	Gearbox under range of loads; no oil
Test 9	Lab	PCB HF	Ring gear	Gearbox under range of loads; no oil

[a] First two tests to compare between gearbox with and without oil, rests are without oil.

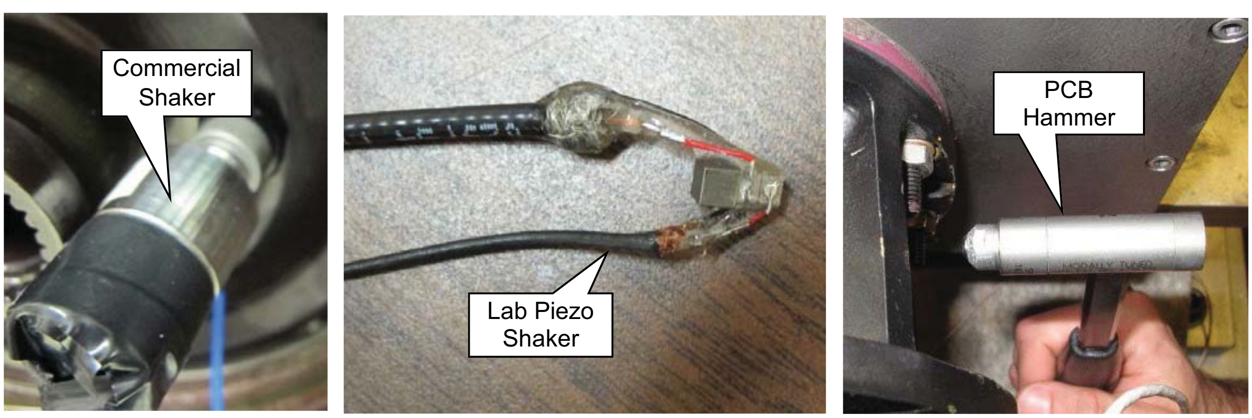

Figure 4.—Two shakers and a hammer used in the tests.

TABLE II.—RANGE OF LOADS APPLIED ON GEARBOX DURING TESTS (REF.10)

Horsepower, %	Torque, in*lb
4	188
9	421
20	939
50	2346
70	3285
100	4693
107	5020
114	5348

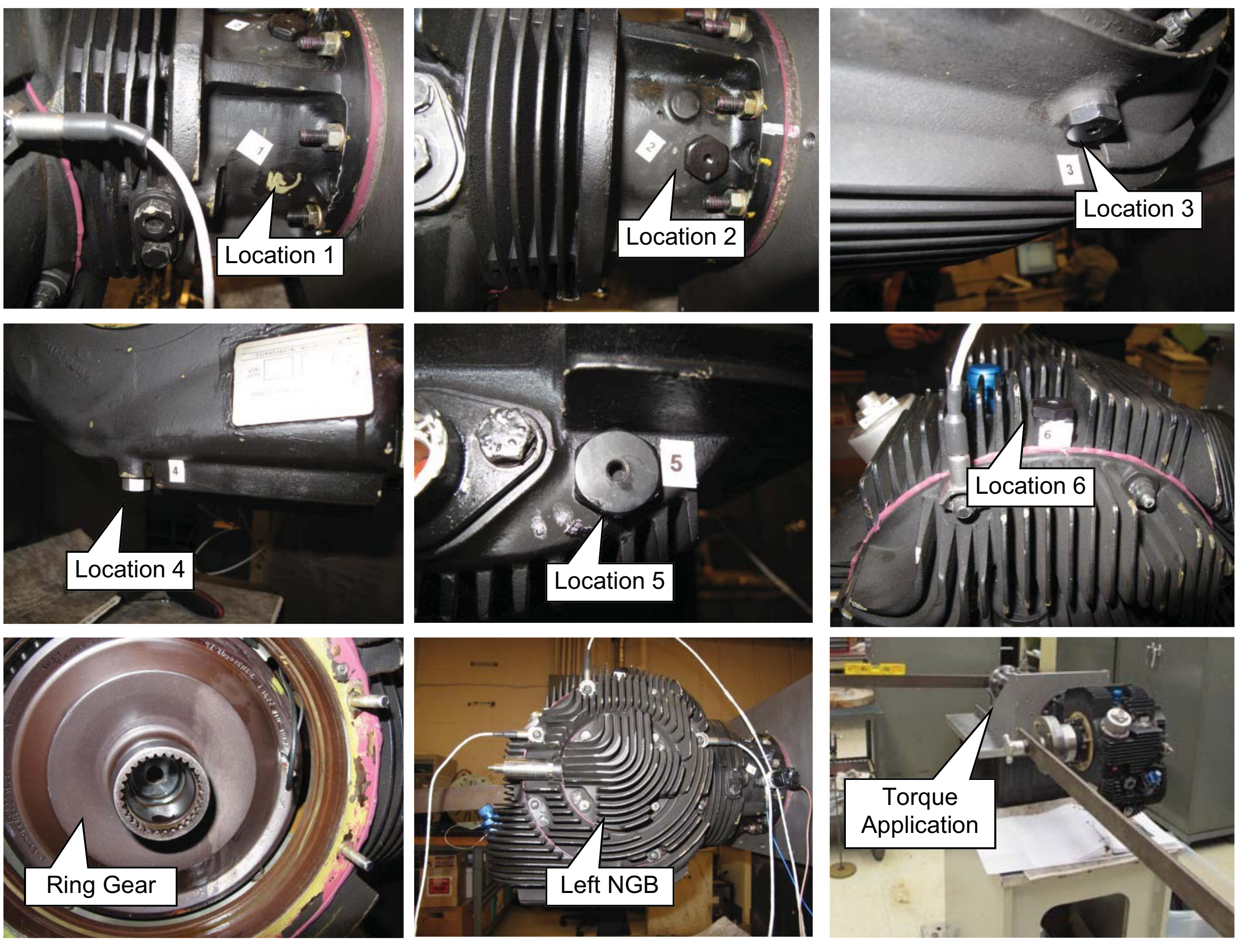

Figure 5.—Shaker locations 1 through 6 in NGB fixture and torque application.

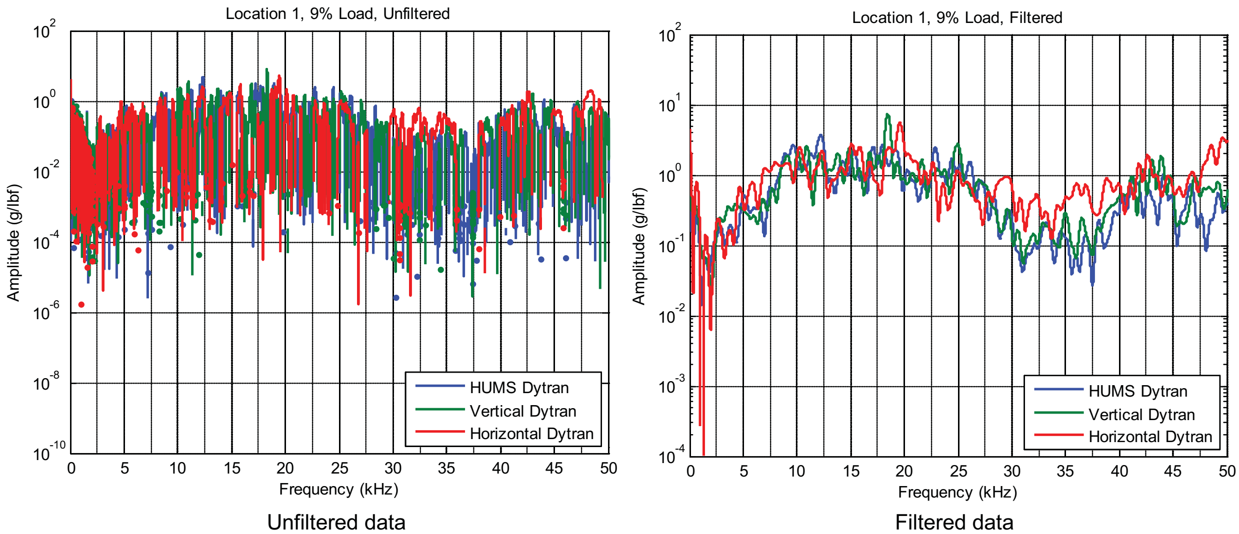

Figure 6.—FRFs before and after filtering.

Results and Discussions

In order to make the FRF plots easier to analyze and compare, a smoothing process was applied to the FRF data. Rather than displaying every ‘blip’ in the measured FRFs, smoothing allows easier viewing and comparison of general vibration transfer path trends. Smoothing preserves the general shape, simplifies the graphs, and makes trend comparisons easier. Figure 6 shows an example of a set of as-measured FRFs as well as the smoothed FRFs from measurements taken on the NGB test fixture (Ref. 9). The results and observations from the measured FRFs are discussed below.

Vibration Transfer Path Consistency

The investigation of similarities/differences and characterization of on-aircraft NGB transfer path dynamics and test-rig dynamics requires that the measured FRFs on the NGB in the lab are comparable to those recorded on the aircraft. The first part of this testing was to demonstrate the similarity/difference between NGB FRFs measured in the lab and those measured on the aircraft. Figure 7 shows the filtered FRFs of the response of the HUMS Dytran accelerometers for all six shaker locations in both NGBs in the helicopter and the left NGB on the test fixture (at 4 percent load).

Across all six test locations, the FRFs compare very well, especially at lower frequency up to 25 kHz, as shown in Figure 7. At the higher frequency, the FRF amplitudes tend to vary between gearboxes sometimes by more than an order of magnitude, and Location 6 especially shows very substantial differences in amplitudes at frequencies over 25 kHz. For the purpose of selecting frequency bands for enveloping/demodulation, these FRF amplitudes overall seem very much similar under frequency of 25 kHz. Table III shows a similarity matrix of Kolmogorov-Smirnov (K-S) tests between FRF amplitude curves for left NGB in the helicopter and test fixture (at 4 percent load).

TABLE III.—K-S SIMILARITY TESTS FOR FRFS AT ALL SIX LOCATIONS

Location	K-S similarity factor
1	0.88
2	0.84
3	0.77
4	0.81
5	0.84
6	0.56

The K-S test is a nonparametric test for the equality of continuous, one-dimensional probability distributions that can be used to compare two samples. The K-S statistic quantifies a distance between the empirical cumulative distribution functions (CDF) of two samples. The two-sample K-S test is one of the most useful and general nonparametric methods for comparing two samples, as it is sensitive to differences in both location and shape of the CDF of the two samples (Ref. 12). The K-S statistic, $\mathrm{D}_{n,n'}$ is defined by Equations (1) and (2).

$$\mathrm{D}_{n,n'} = sup_x|F_{1,n}(x) - F_{2,n'}(x) \tag{1}$$

$$F_n(x) = \frac{1}{n}\sum_{i=1}^{n} I[X_i \leq x] \tag{2}$$

Where, sup_x is the supremum (greatest) distance between the empirical distribution functions $F_{1,n}$ and $F_{2,n'}$ of the first and second samples, respectively, and $I[X_i \leq x]$ is the indicator function equal to 1 if $X_i \leq x$, or 0 otherwise. In K-S tests, factor $\mathrm{D}_{n,n'}$ represents the maximum vertical distance between the CDF curves of two comparable vectors (herein FRF amplitudes for helicopter and test fixture). K-S Similarity Factors between the FRF vectors in Table III were derived by subtracting $\mathrm{D}_{n,n'}$ from the unity. Figure 8 shows CDF plots of FRF amplitudes for shaker Location 1 to 6 in left NGB in helicopter and test fixture. According to Table III, FRF curves for Locations 1 to 5 show 77 to 88 percent similarity while that in Location 6 has only 56 percent similarity with a difference in amplitudes of approximately 10 g/lbf.

Since no internal measurements were made on the helicopter at gear mesh, a comparison of external measurements within a frequency band known to contain gear mesh dynamics was made. Figure 9 shows FRF comparison with coherence and CDF plots for K-S test results within the frequency band that contains ±3 sidebands around the gear mesh for Commercial Shaker at Location 1 of left NGBs in NASA and on the helicopter under minimal load conditions. Coherence is the linear dependence between the output and input signals as a function of frequency. The comparison shows a 66 percent similarity between the FRFs of left NGBs in NASA and helicopter within this frequency band of interest. However, gear CIs are measured under load conditions and the effect of load on response will be discussed in two following sections. The plot also indicates the helicopter values are greater for the cumulative fraction. Overall, it can be concluded that vibration transfer paths are consistent in NGBs between the helicopter and test fixture.

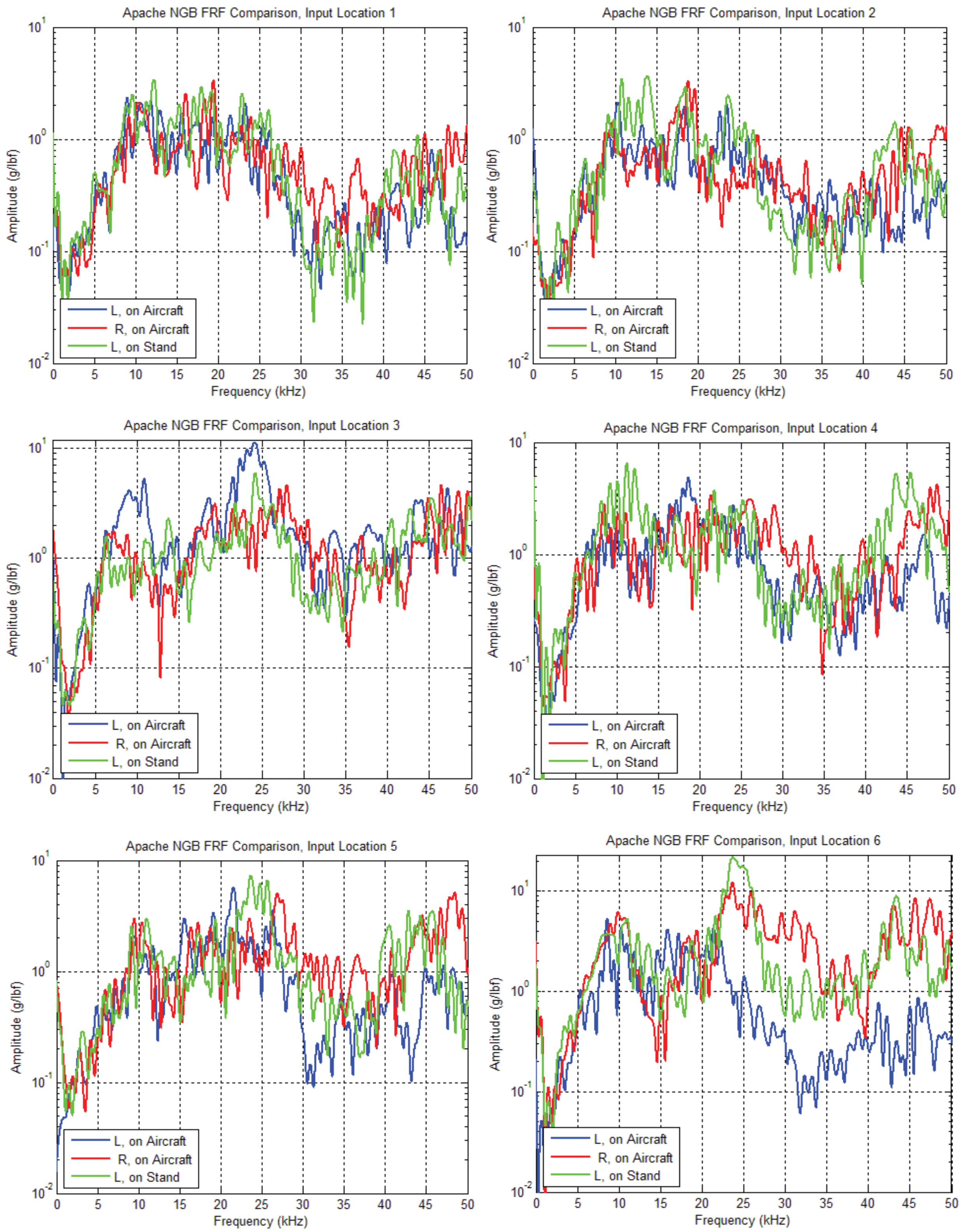

Figure 7.—FRFs and Coherence comparisons at six locations of NGBs in test fixture and helicopter.

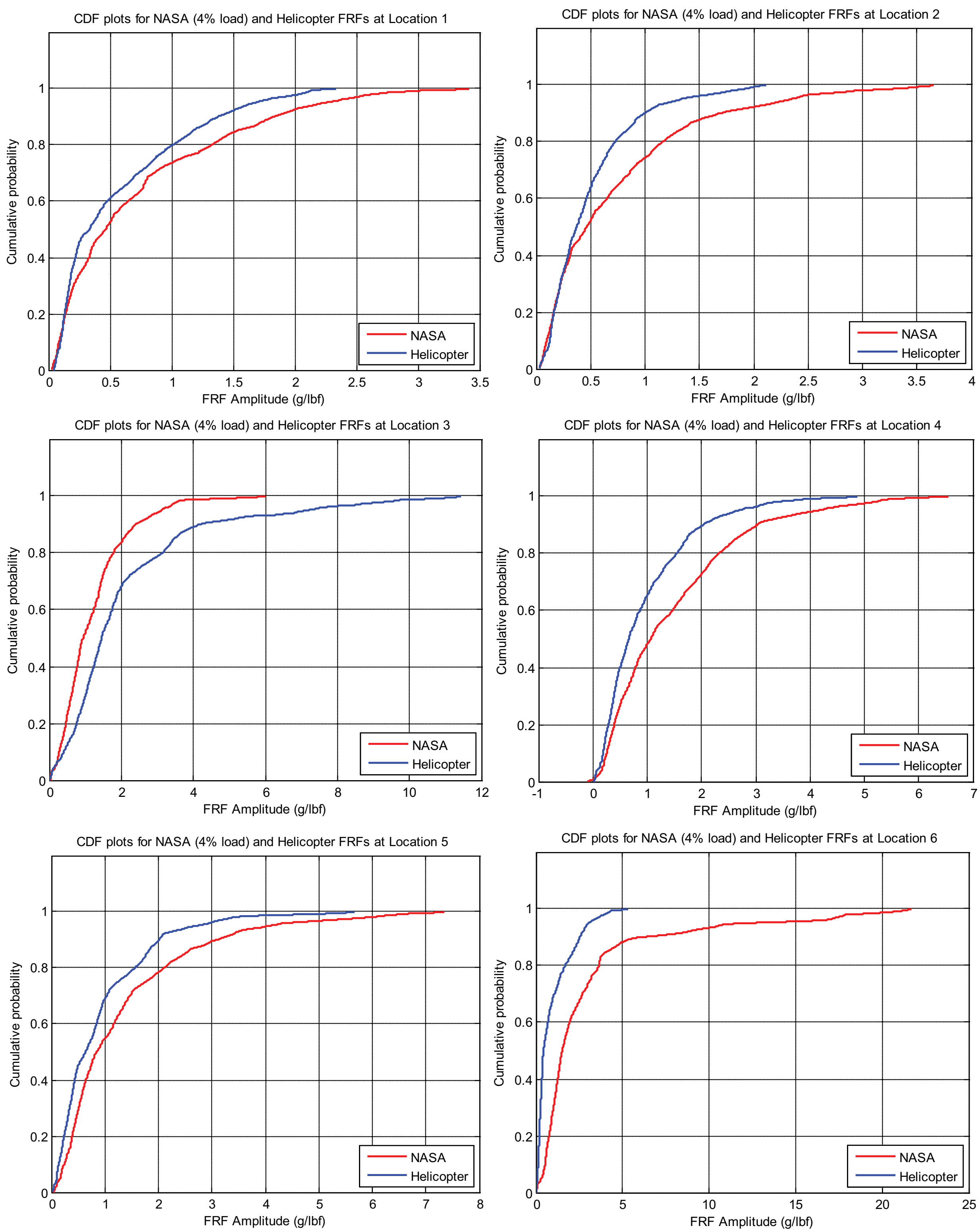

Figure 8.—CDF plots for Com. Shaker at six locations of NGBs in test fixture and helicopter.

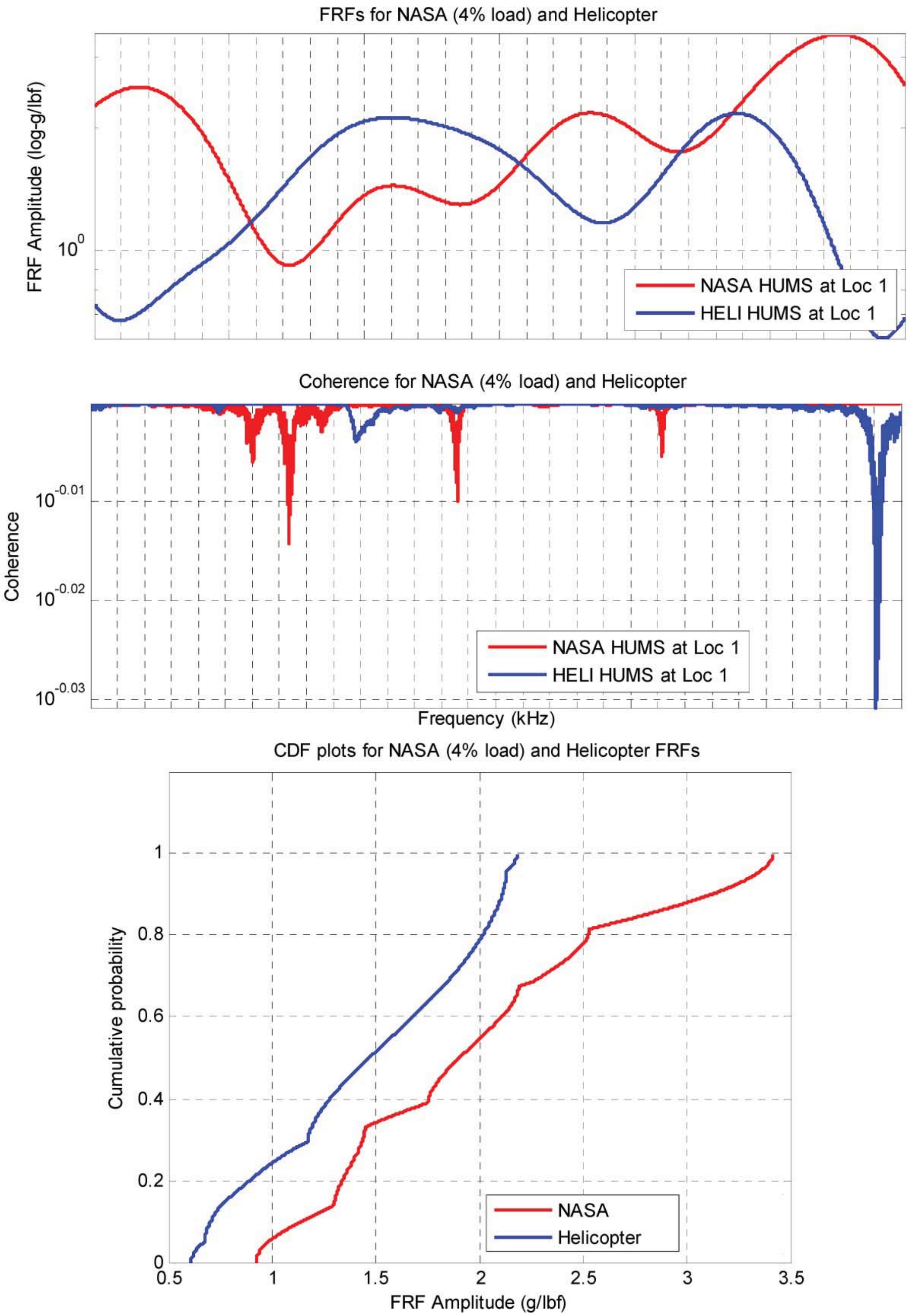

Figure 9.—FRFs, coherence and CDF plots for Commercial Shaker at Location 1 of NGBs in test fixture helicopter.

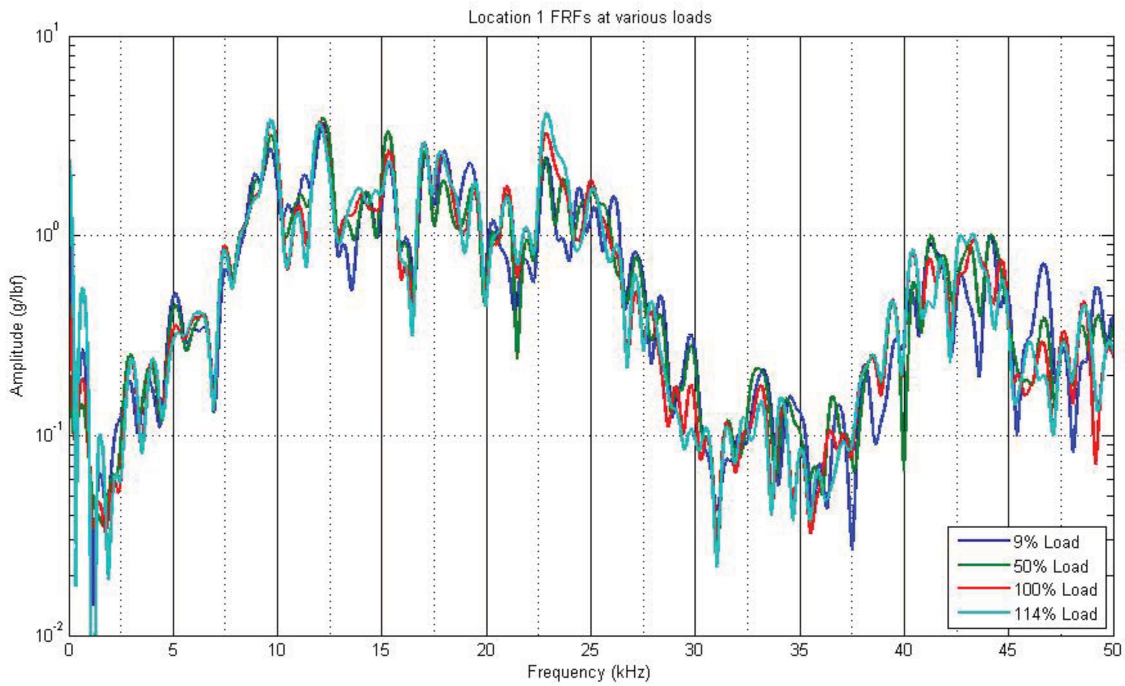

Figure 10.—FRFs for Com. Shaker at Location 1 of NGB fixture under various loads.

Bearings Under Varying Loads

A helicopter gearbox is subjected to widely varying loads in normal operation; therefore, it is important to understand the gearbox's transfer path characteristics in such cases. Substantial changes in transfer path with load may indicate that the regime recognition is critical for reliable health monitoring. The vibration transfer path was measured in the lab NGB with the shaker at Location 1 and the gearbox under a range of torques indicated by a percent of the gearbox's maximum torque rating. In total, the gearbox was tested under these conditions at eight different torque percentages shown in Table II; however, in the interest of clarity, only four are shown in Figure 10. The pictured FRFs match each other very well through the first 30 kHz frequency and are still easily comparable beyond that. This test illustrates that the surface-measured vibration transfer path measured under static conditions in the NGB subjected to considerably variable torque under operating conditions will not change significantly. Additionally, this type of measurement was also made previously on an AH-64 intermediate gearbox (IGB) with a specialized bearing transducer and produced similar results (Ref. 8). Therefore, it appears that the bearing vibration transfer paths measured on the external NGB surface, under static conditions, are not much affected by variations in gearbox loads.

Gears Under Varying Loads

While the bearing vibration transfer path changes very little under variable loading conditions, the gear vibration transfer path changes more with loads, as shown in Figure 11. The figure shows FRFs under 4 and 107 percent torque loads from excitation with the lab piezoshaker at the ring gear. Table IV shows a similarity matrix of K-S tests between FRF amplitude curves for the test fixture between 4 percent load and six other loads from 0 to 50 KHz. The K-S Similarity factor decreases as the load increases.

This fact suggests that the contact stress at the gear mesh plays a significant role. As larger torque is applied to the input shaft of the gearbox, the contact area between the gear and pinion teeth in mesh increases slightly changing the vibration transfer path. The likely reason that the surface or bearing transfer paths do not change much with load is that the transfer path for bearings is through the outer race, the housing, and then to the sensor, and not dependent on stress due to change in contact area in the gear mesh. With gears, however, the energy must pass through the bearings and the gear teeth before being transmitted to the case. It seems likely that small changes in contact area and contact stress in the gear mesh would affect the vibration transfer path more noticeably. By extension, it seems likely that the vibration transfer path for a bearing fixed race defect may also be load-dependent since it is directly connected to the gear. It is important to note that while the gear transfer paths are more load dependent, they do no differ much more than those seen on different gearboxes. As a result, the same frequency band would likely be chosen for health monitoring for all load cases; however, certain condition indicator amplitudes at some frequencies may change significantly. This effect suggests that regime recognition may be important for reliable condition indicators of gear health. Therefore, a separate future study of different gear CIs measured during rotating conditions is required to determine their response to torque changes. However, a brief discussion of the similarity within a narrow band of interest will be discussed in a following section.

TABLE IV.—K-S SIMILARITY TESTS FOR FRFS AT SIX LOADS COMPARED TO 4 PERCENT LOAD

Horsepower, %	Torque, in*lb	K-S similarity factor
9	421	0.95
20	939	0.91
50	2346	0.89
70	3285	0.88
100	4693	0.87
107	5020	0.86

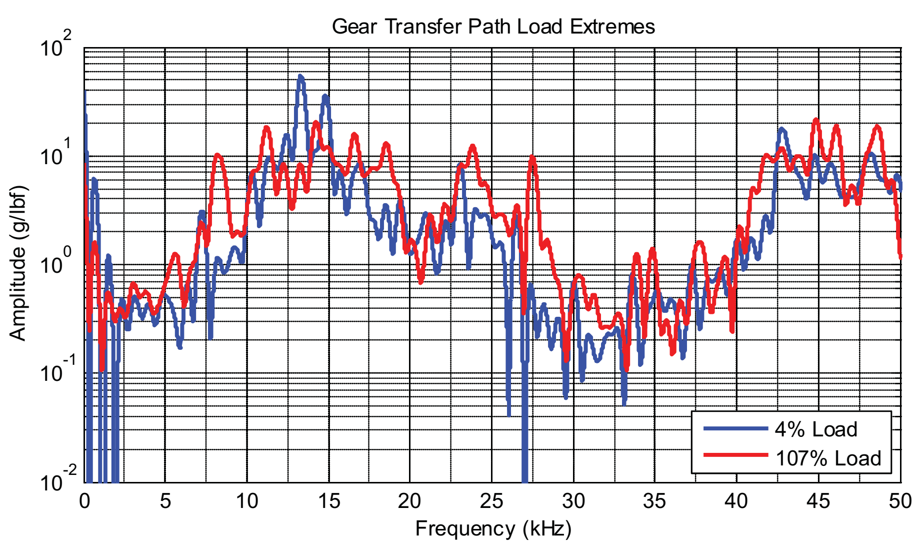

Figure 11.—HUMS FRFs with Lab Piezo Shaker on ring gear under various loads.

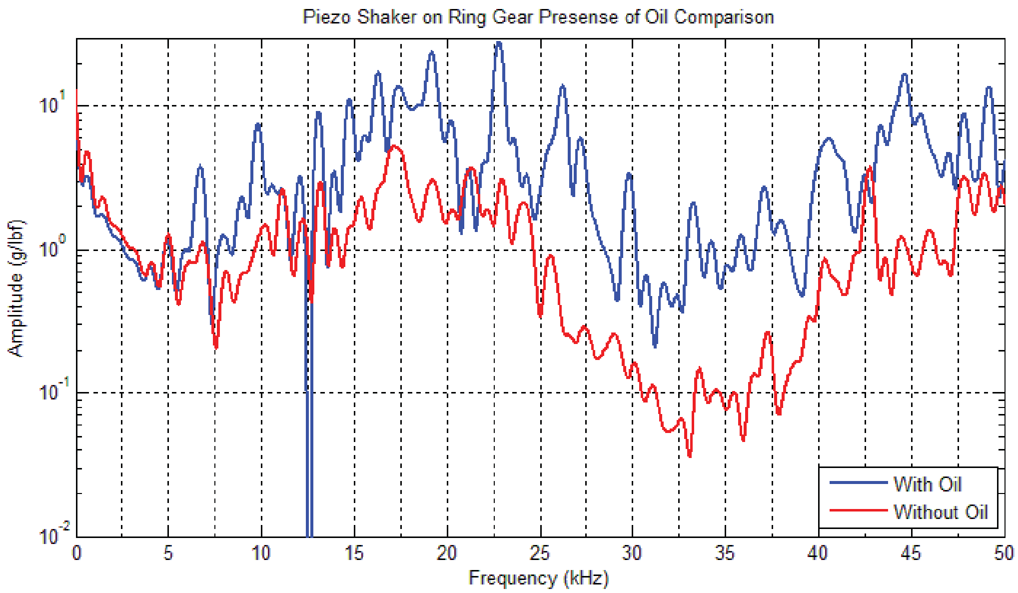

Figure 12.—FRFs with Lab Piezo Shaker on ring gear for gearbox with and without oil.

Presence of Lube Oil

While the helicopter NGB is operating, the oil pump will be engaged in circulating oil within the gearbox. It is impossible to exactly replicate these circumstances in the lab without the means of controlling the pump; therefore, as a compromise, vibration transfer path measurements were recorded in the two extreme conditions: the gearbox full of oil and the gearbox without oil. The reason for taking such measurements under these two extreme conditions is the initial perception that the vibration transfer path of the gearbox in operation will be somewhere between these two extreme situations. In fact, the measurements taken on the helicopter were recorded with the gearbox full of oil; though they were external measurements and not likely to be strongly affected by the presence of oil.

Figure 12 shows that the addition of oil into the gearbox quite significantly increases the amplitude of FRFs from the Lab Piezo Shaker on the ring gear to the accelerometers mounted on the outside of the gearbox. This might be due to the oil resting at the bottom of the gearbox acted as an additional medium for the transfer of vibrational energy. This does not happen if there is no oil present at the bottom of the gearbox. However, despite the transfer path improvement due to oil at the bottom of the gearbox, it is realistic to assume that the ‘gearbox without oil’ condition more closely resembles the gearbox under actual operating conditions since most of the oil in the gearbox would be circulated by the oil pump rather than resting at the bottom.

Sensor Orientation and Removal/Replacement

While HUMS is a sophisticated system, its components undergo real world maintenance treatments that may not be ideal. During these tests, some of these real world conditions were recreated in the lab to investigate if they have any detrimental effects on the system performance. These varying maintenance conditions include skewing or clocking the accelerometer by changing its angle relative to the gearbox, as well as removing and reattaching it.

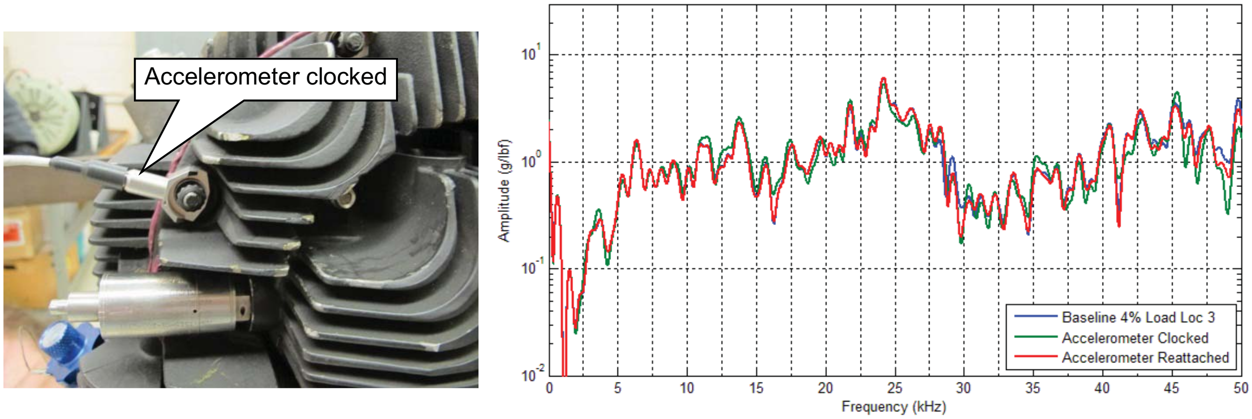

(a) (b)

Figure 13.—Commercial shaker at Location 3 of NGB fixture with varying maintenance conditions.

For this comparison, the test with the gearbox under 4 percent load and the shaker at Location 3 were used as a baseline. The nut holding the HUMS accelerometer in place was loosened and the accelerometer was rotated clockwise so that the angle between its direction of sensitivity and the gearbox's horizontal was approximately 30°, which can be seen in Figure 13(a). The condition of removal and reattachment of accelerometer was also tested by completely removing the nut and the accelerometer, and then reattaching them with a combination wrench, tightening the nut to an unknown torque. This condition was worth testing because the HUMS Dytran accelerometer documentation specifies that the sensor should be held in place with a nut under a specific torque. Figure 13(b) clearly shows that the varying some maintenance conditions of the HUMS Dytran accelerometer do not detrimentally affect the accelerometer performance.

Alternate Accelerometer Locations

The existing helicopter HUMS uses a single Dytran accelerometer mounted on a stud forward on the gearbox. It is not known exactly why this location was chosen. Therefore, two other Dytran accelerometers were mounted on the gearbox in different locations to explore the possibility of other accelerometer locations being more suitable/effective for detecting defects. The two additional locations, 'Vertical' and 'Horizontal' at approximately right angles to each other and the original HUMS location are shown in Figure 14(a). The 'Vertical' accelerometer location was chosen because it may measure response that is orthogonal to the HUMS accelerometer's direction, and thus in the direction of gear mesh. The 'Horizontal' accelerometer location was chosen because it was closer to the input bearing, and much closer to the gear mesh of the gearbox than the HUMS accelerometer, thus it may be able to better capture defect signals from those locations.

Figure 14(b) shows the FRFs from all three Dytran accelerometer locations under 4 percent load. Clearly, there is very little difference in FRFs measured from these three locations. Though not expected, it appears that the transfer path from the gear-mounted shaker to the studs on the outer casing does not significantly change between studs. In order to understand this, the somewhat radially symmetric nature of the gearbox needs to be taken into account. When examined closely, it became evident that the shortest path from the outer circumference of the gear to any point on the outer circumference of the gearbox access cover is always at the center of the gear through the output shaft to the center of the access cover, and then out to the circumference of the cover. This is likely to be the reason for the FRF similarity between different accelerometer locations.

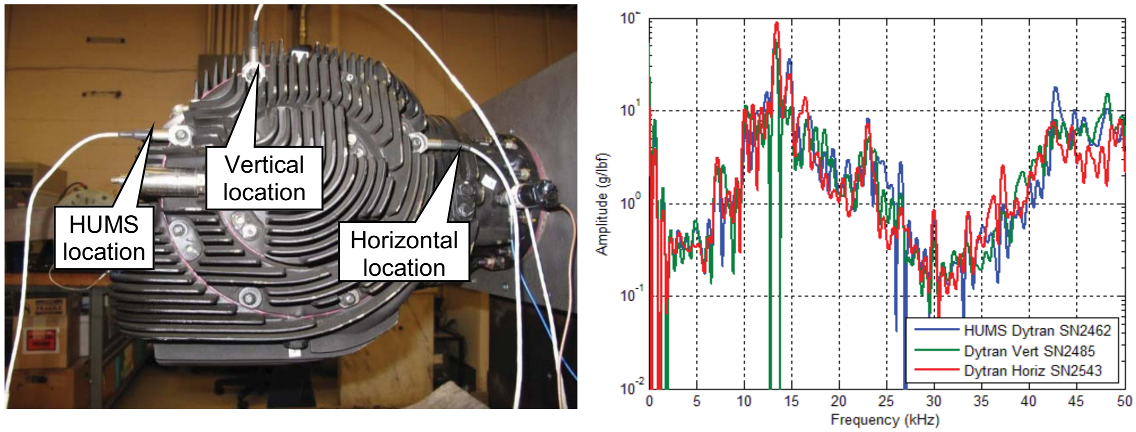

(a) (b)

Figure 14.—Sensor locations comparison at 4 percent load with Lab Piezo Shaker on ring gear.

Lightly-Damped Steel Gear

The VTPs measured for bearings are through the cast aluminum alloy gearbox cases, and this material is generally highly damped. When the case was struck with a hammer, the sound was a thud and decayed very quickly. On the other hand, the steel gear rings more like a bell when struck. This audible difference is a macroscopic indication of one of the physical characteristics of gears that may impede gear health monitoring. This characteristic was investigated by measuring the transfer path from a point on the ring gear to another point on the gear, and to the standard acceleration location. The test setup with upper and lower accelerometers on the ring gear is shown in Figure 15(a). The notable trait of the FRFs measured with the Lab Piezo Shaker mounted directly on the ring gear is the sharp resonances seen in Figure 15(b). These FRFs were measured with the cover off and the blue trace is generated from the response of the accelerometers mounted directly on the ring gear, and the green trace is produced from the HUMS accelerometer mounted on the stud. The blue trace, which shows the direct FRFs of the ring gear, indicates a lightly-damped structure. FRFs measured on this type of structure tend to have much sharper and closer resonances and anti-resonances, while the green trace which shows the VTP to the HUMS accelerometer shows the characteristics of a structure which has high damping, and the FRFs tend to have softer, more spread-out resonances and anti-resonances. However many of the sharp peaks seen in the blue trace are still visible in the green indicating that the dynamics of the gear itself play a significant role in determining the gear mesh transfer path. For health monitoring, the broad, highly-damped peaks provide more consistent energy transmission through a frequency range, while the sharp, lightly-damped peaks provide high amplification, but over a very short frequency range. These lightly-damped peaks have some implications for health monitoring—relatively small changes in frequency may produce large changes in amplitude, which will affect the gear CIs response. While helicopter drivetrains are run at a constant speed, the frequencies at these peaks will likely vary between gearboxes and may produce large amplitude differences between helicopters. This further highlights the need to run a test rig at varying conditions to assess CI performance.

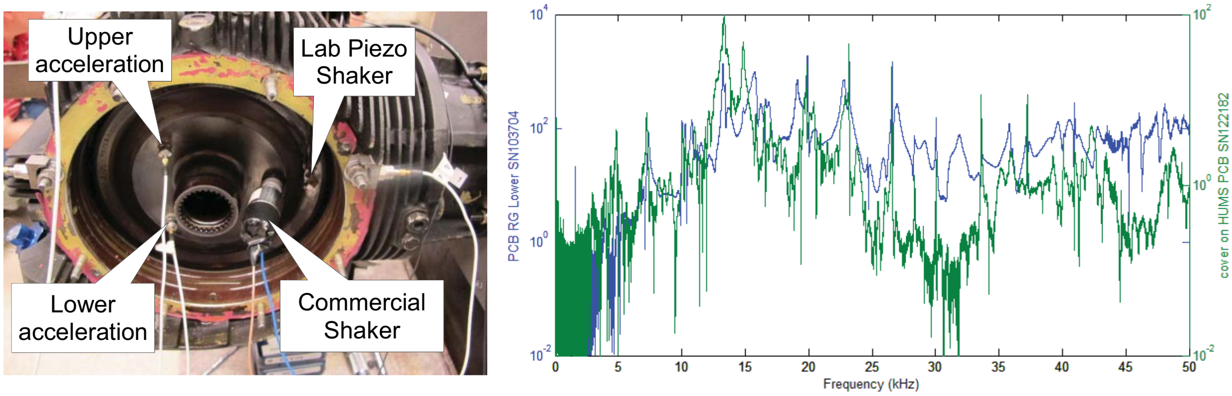

(a) (b)

Figure 15.—FRFs comparison between accelerometers mounted on ring gear and housing.

Sensor Dynamics

The Dytran accelerometers used to monitor the helicopter NGB have an integral mounting bracket. While the sensor itself is supposed to provide flat response to 5 kHz with its first resonance at 26 kHz, the mounting bracket has structural modes beginning at 3 kHz. High-frequency monitoring including enveloping or demodulation is performed above 5 kHz; therefore, the bracket dynamics play a part in the measured response. To separate the bracket dynamics from the sensor dynamics, the Dytran accelerometers were replaced with high frequency PCB accelerometers attached to mounting brackets, which were made to emulate the Dytran brackets. Although the Dytran accelerometers used on the HUMS systems are not likely to be replaced anytime in the near future, the Spiral Bevel Gear Test rig has Dytran accelerometers as well as lab-grade sensors, and therefore, this data may be useful in creating a more meaningful comparison of vibration transfer paths between Spiral Bevel Gear Test Rig and the helicopter.

Figure 16 shows these unfiltered FRFs with the corresponding coherence graph. In general, the FRFs are similar, but the PCB accelerometers appear to provide better-quality measurements, as evidenced by the cleaner FRFs and superior coherence. The primary difference in these sensors can be seen in the 42 to 50 kHz region, where the Dytran accelerometer's response is an order of magnitude higher than that of the PCB accelerometer. This seems to suggest that the Dytran accelerometer is receiving additional amplification in this region, perhaps from a bending mode of the mounting bracket or a sensing element resonance.

Future Comparison to the Spiral Bevel Gear Fatigue Test Rig

One underlying objective of the FRF measurements is to determine if measuring the behavior of the structure under static conditions can provide any insight into CI performance across three spiral bevel geared systems: the helicopter NGB, NGB fixture and Spiral Bevel Gear Fatigue Test Rig. This requires first making measurements on the helicopter or fixture that can be compared to future measurements on the test rig. Limited accessibility to the gear mesh within the NGB installed on the helicopter made it impossible to simulate an impact of the gear teeth at the source. However, measurements made with the actuator on the ring gear banded at gear mesh frequencies at specific torques could be compared to the response of the actuator installed on the ring gear within the test rig banded around its gear mesh frequencies at specific torques.

FRFs and coherence were measured by the Dytran accelerometer with the shaker on the ring gear, at a frequency band that contains ±3 sidebands around the gear mesh. These measurements were taken at six loads and compared to the 4 percent load conditions. These plots and the corresponding CDF plots for the six loads are shown in Figure 17 and Figure 18. Table V shows a similarity matrix of K-S tests between FRF amplitude curves for the test fixture between 4 percent load and six other loads within this frequency band. The K-S Similarity factor within this narrow frequency band improves at the higher loads. The coherence also improves with higher loads. The shape of the signature also changes at higher loads. This illustrates the importance of assessing the similarities of frequency response within frequencies of interest. Measurements will be made in the Spiral Bevel Gear Fatigue Test Rig under comparable conditions in future studies and then compared to dynamic conditions for the helicopter and test rig to determine how CI performance is related to VTP amplitude with the rig at static conditions.

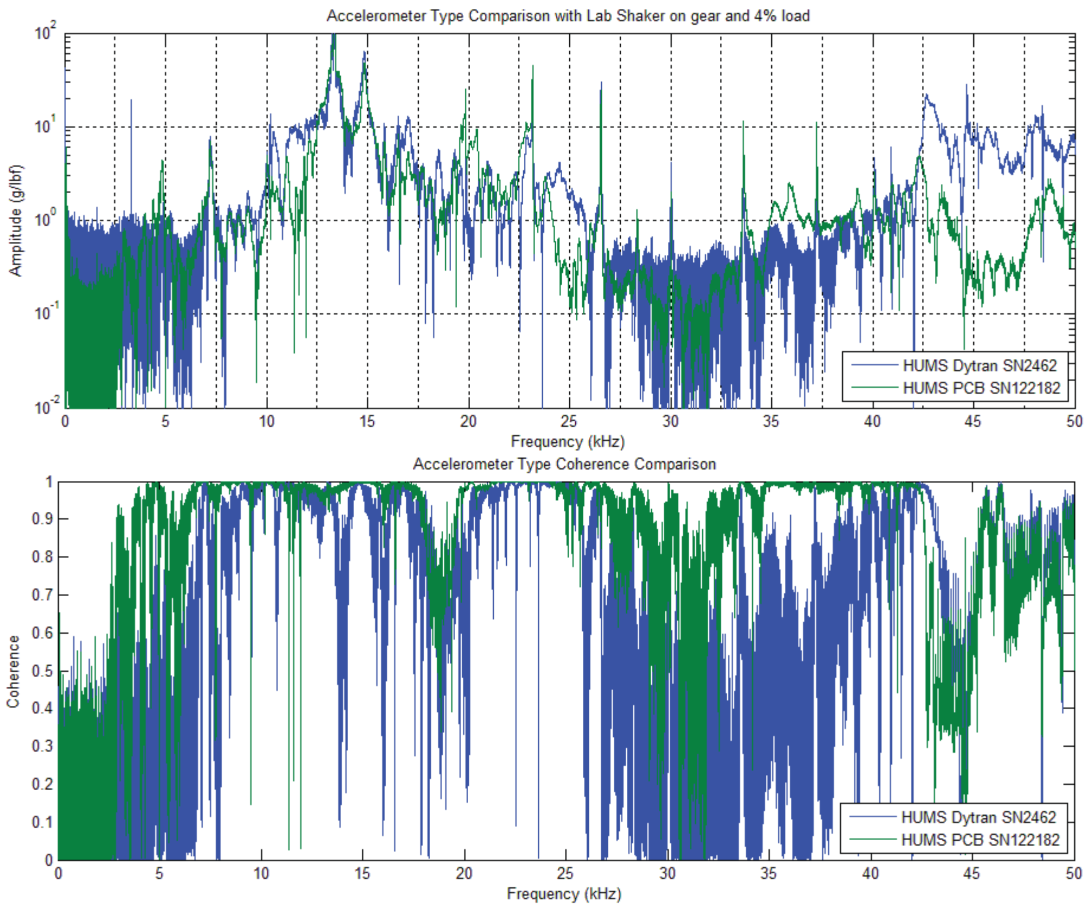

Figure 16.—Sensor type comparison at 4 percent load with Lab Piezo Shaker on ring gear.

TABLE V.—K-S SIMILARITY TESTS FOR FRFS AT SIX LOADS COMPARED TO 4 PERCENT LOAD WITHIN A FREQUENCY BAND

Horsepower, %	Torque, in*lb	K-S similarity factor
9	421	0.83
20	939	0.68
50	2346	0.74
70	3285	0.88
100	4693	0.87
107	5020	0.87

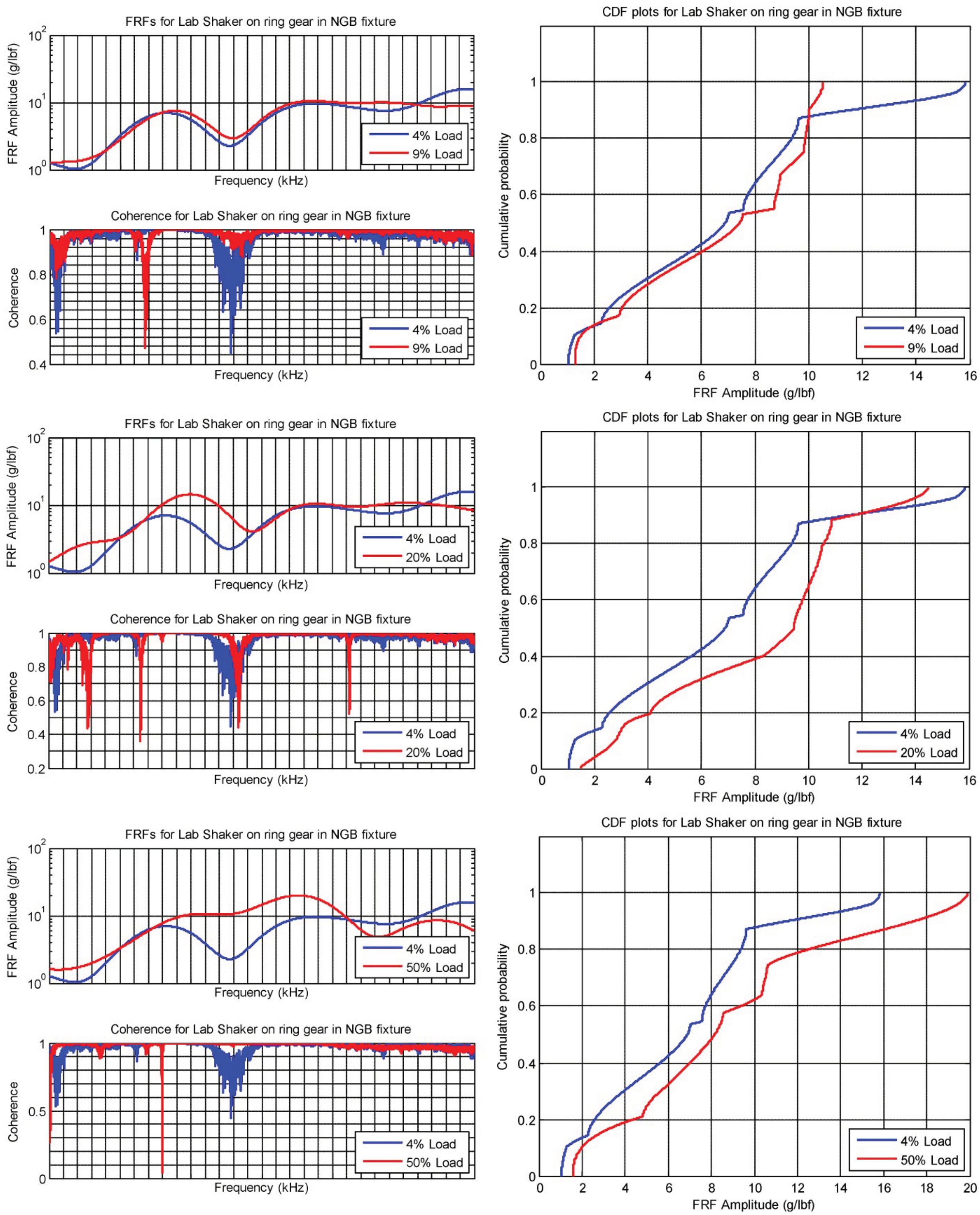

Figure 17.—HUMS FRFs, Coherence and CDF at 9, 20 and 50 percent loads compared to 4 percent.

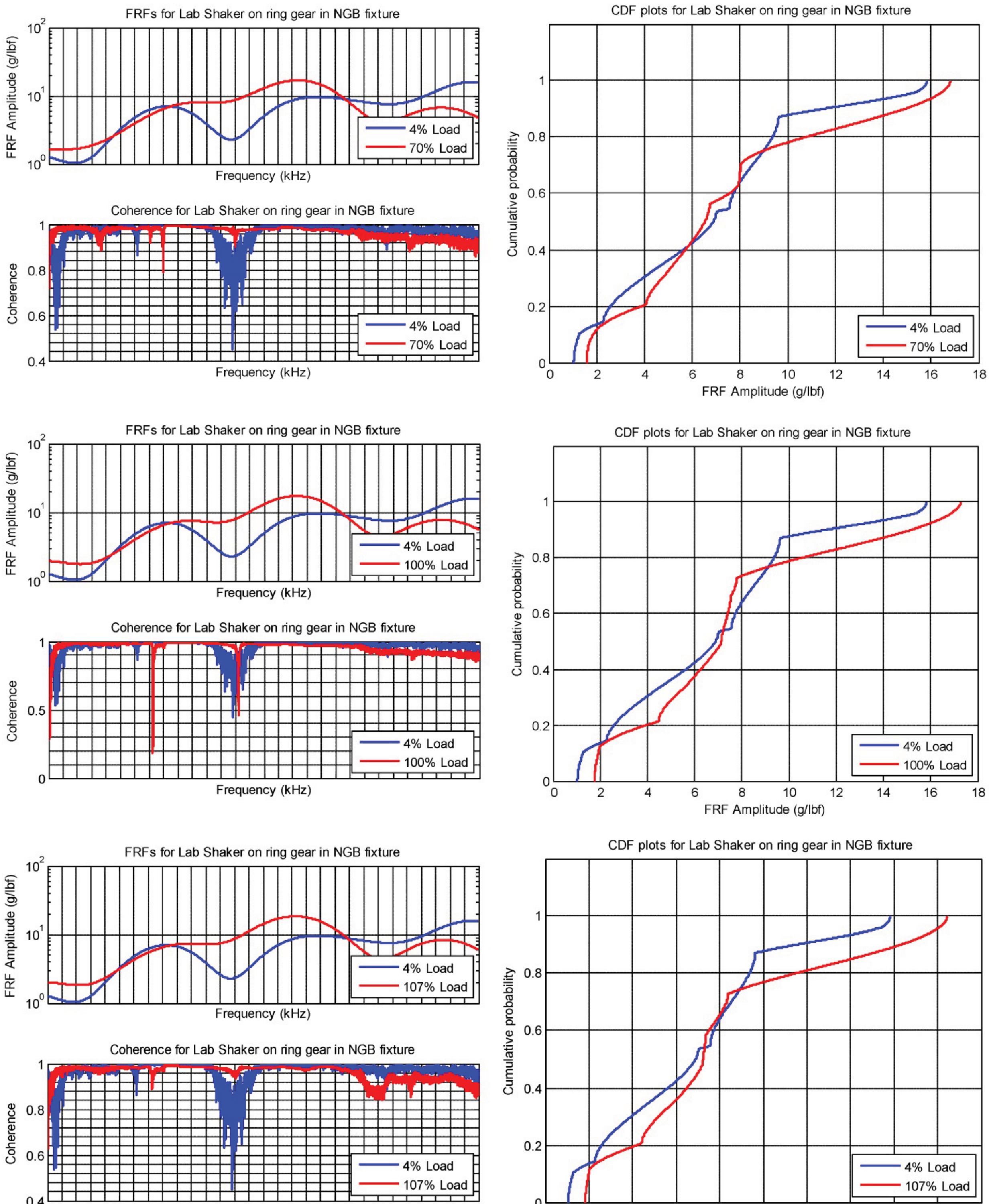

Figure 18.—HUMS FRFs, Coherence and CDF at 70, 100 and 107 percent loads compared to 4 percent.

Summary and Conclusions

The measurements taken on the test fixture nose gearbox at GRC were shown to be consistent with those taken on similar gearboxes mounted in an AH-64 helicopter. It was also shown that certain real world installation and maintenance issues, such as sensor alignment and installation torque, do not significantly affect the performance of HUMS. It has been shown that the presence of oil increased the amplitude of FRFs at some frequencies through acting as an additional medium for vibrational energy transfer. However, the no-oil condition is closer to real world conditions in a running aircraft, since the oil would be circulated by the oil pump rather than resting at the bottom. In fact, oil only affects the gear VTP, not the bearing VTP. It was also found that neither of the alternative accelerometer locations showed any marked improvement in vibration energy transmissibility from the ring gear.

Gear vibration transfer path dynamics are found to be load dependent to some extent and depends on the frequency of interest. The replacement of Dytran accelerometers with PCB high frequency sensors provided cleaner data. The lightly-damped ring gear produced sharp and closer transfer path resonances and anti-resonances, and these may lead to substantially different condition indicator amplitudes with changing operating conditions, or even between gear boxes with different serial numbers. Ultimately, the test diagnostician must understand these differences and make every attempt to develop algorithms, which are robust to the actual conditions found on the aircraft. The key to improving CI performance across systems (helicopter, fixture, test rig) is to understand dynamic characteristics unique to each system that affect individual gear CI response for a healthy and damaged tooth. Therefore, the vibration transfer path characterization and consistencies found in this research might be useful in characterizing differences/ similarities in structural dynamics between a test rig and a helicopter, and their effects on gear CI performance.

References

1. Dempsey, P. J., Lewicki, D. G., and Le, D. D., "Investigation of Current Methods to Identify Helicopter Gear Health," IEEE Aerospace Conference, Big Sky, Montana, March 3-10, 2007.
2. Aviation Safety and Security Program, the Helicopter Accident Analysis Team, "Final Report of the Helicopter Accident Analysis Team," 1998.
3. Learmount, D., Rotary Woes, Flight International, no. 4725, vol. 157, pp. 34–35, 2000.
4. Romero, R., Summers, H., and Cronkhite, J., "Feasibility Study of a Rotorcraft Health and Usage Monitoring System (HUMS): Results of Operators Evaluation," NASA CR–198446, ARL-CR-289, DOT/FAA/AR-95/50, February 1996.
5. Dempsey, P. J., Brandon, E. B., "Validation of Helicopter Gear Condition Indicators Using Seeded Fault Tests," NASA/TM—2013-217872, April 2013.
6. Antolick, L. J., Branning, J. S., Wade, D. R., and Dempsey, P. J., "Evaluation of Gear Condition Indicator Performance on Rotorcraft Fleet," American Helicopter Society 66th Annual Forum Proceedings, Phoenix, Arizona, May 11-13, 2010.
7. Delgado, I. R., Dempsey, P. J., Antolick, L. J., and Wade, D. R., "Continued Evaluation of Gear Condition Indicator Performance on Rotorcraft Fleet," American Helicopter Society Condition Based Maintenance Specialist Meeting, February 2013.
8. Wade, D., and Larsen, C., Roth, R., and Shelley, S., Final Report of Bearing Condition Indicator Refinement Project, Technical Report Rdmr Ae-06-01, June 2011.
9. Feldman, J. and Larsen, C., Apache Left Nose Gearbox Transfer Path Measurements. Etegent Technologies Contract Report prepared for NASA Glenn Research Center. May 2012.
10. General Electric Company. Advertisement. *T700/CT7 Engine Family*. GE Aviation, 2012. Web. 11 July 2013.
11. PCB Piezotronics, Depew, New York, http://www.pcb.com/. Accessed September 6, 2013.
12. Massey, F. J. "The Kolmogorov-Smirnov Test for Goodness of Fit," Journal of the American Statistical Association. Vol. 46, No. 253, 1951, pp. 68–78.